Published in final edited form as:

Mol Cell. 2017 July 06; 67(1): 44–54.e6. doi:10.1016/j.molcel.2017.05.035.

A novel RNA phosphorylation state enables 5′-end-dependent degradation in *Escherichia coli*

Daniel J. Luciano[1,2], **Nikita Vasilyev**[3], **Jamie Richards**[1,2], **Alexander Serganov**[3], and **Joel G. Belasco**[1,2,*]

[1]Kimmel Center for Biology and Medicine at the Skirball Institute, New York University School of Medicine 540 First Avenue, New York, NY 10016, USA

[2]Department of Microbiology, New York University School of Medicine 540 First Avenue, New York, NY 10016, USA

[3]Department of Biochemistry and Molecular Pharmacology, New York University School of Medicine 540 First Avenue, New York, NY 10016, USA

SUMMARY

RNA modifications that once escaped detection are now thought to be pivotal for governing RNA lifetimes in both prokaryotes and eukaryotes. For example, converting the 5′-terminal triphosphate of bacterial transcripts to a monophosphate triggers 5′-end-dependent degradation by RNase E. However, the existence of diphosphorylated RNA in bacteria has never been reported, and no biological role for such a modification has ever been proposed. By using a novel assay, we show here for representative *Escherichia coli* mRNAs that ~35–50% of each transcript is diphosphorylated. The remainder is primarily monophosphorylated, with surprisingly little triphosphorylated RNA evident. Furthermore, diphosphorylated RNA is the preferred substrate of the RNA pyrophosphohydrolase RppH, whose biological function was previously assumed to be pyrophosphate removal from triphosphorylated transcripts. We conclude that triphosphate-to-monophosphate conversion to induce 5′-end-dependent RNA degradation is a two-step process in *E. coli* involving γ-phosphate removal by an unidentified enzyme to enable subsequent β-phosphate removal by RppH.

eTOC blurb

*Corresponding author and Lead contact: joel.belasco@med.nyu.edu.

AUTHOR CONTRIBUTIONS

D.J.L., N.V., J.R., A.S., and J.G.B. designed the experiments, D.J.L., N.V., and J.R. conducted the experiments, and D.J.L., N.V., J.R., A.S., and J.G.B. interpreted the data and wrote the paper.

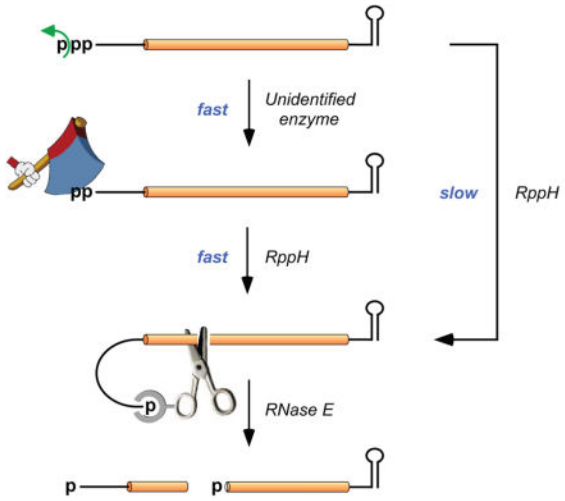

Luciano *et al.* show that diphosphorylated mRNA 5′ ends are abundant in *E. coli* and that the *E. coli* RNA pyrophosphohydrolase RppH prefers diphosphorylated substrates to their triphosphorylated counterparts. Their findings suggest that converting triphosphorylated to monophosphorylated 5′ ends before RNase E cleavage involves sequential phosphate removal by distinct enzymes.

Keywords

Diphosphate; RNA decay; pyrophosphatase; guanylyltransferase; Pce1; cap; PACO; PABLO; transcription initiation; RNA polymerase; *E. coli*; *yeiP*; *metE*

INTRODUCTION

Of the various mechanisms by which genes are regulated, mRNA degradation is among the least well understood. In both eukaryotes and prokaryotes, the lifetimes of individual messages can differ by as much as two orders of magnitude, with proportionate effects on protein synthesis. However, in spite of the widespread regulatory impact of this process, the basis for most differences in mRNA longevity has yet to be explained.

Eukaryotic mRNAs are typically protected from unrestrained degradation by a 5′-terminal cap and a 3′-terminal poly(A) tail, the removal of which is tightly controlled and exposes messages to rapid exonucleolytic destruction (Garneau et al., 2007). By contrast, bacterial mRNAs are thought to be protected by a 5′-terminal triphosphate and a 3′-terminal stem-loop and to be degraded by a distinct set of ribonucleases (Hui et al., 2014). Despite progress toward elucidating mRNA decay in bacteria, many of the most important molecular mechanisms that govern mRNA longevity in such organisms have remained obscure, even in so well studied a species as *Escherichia coli*.

In *E. coli*, mRNA degradation usually proceeds via either of two pathways that both involve cleavage by RNase E, an endonuclease that cuts with only modest sequence specificity in single-stranded regions that are AU-rich (McDowall et al., 1994; Lin-Chao et al., 1994;

Kaberdin, 2003; Del Campo et al., 2015; Chao et al., 2017). In one of these pathways, RNase E gains direct access to internal sites within unprocessed primary transcripts bearing a 5′-terminal triphosphate. Cleavage at these sites produces two fragments: (i) a 5′ fragment that lacks a protective stem-loop at its 3′ terminus and therefore undergoes rapid 3′-exonucleolytic degradation and (ii) a monophosphorylated 3′ fragment that is highly susceptible to further RNase E cleavage due to the preference of this enzyme for substrates that have a single phosphate at the 5′ end (Mackie, 1998). Degradation by the other pathway is 5′-end-dependent, as it is triggered by removal of two of the three phosphates from the 5′ terminus of primary transcripts so as to generate a full-length mRNA that is monophosphorylated and therefore vulnerable to attack by RNase E (Celesnik et al., 2007). Central to this initial triggering event is the RNA pyrophosphohydrolase RppH (Deana et al., 2008).

In vitro, *E. coli* RppH converts triphosphorylated RNA to monophosphorylated RNA in a single step by cutting between the two phosphates (α and β) adjacent to the first nucleoside, generating pyrophosphate as the principal by-product (Deana et al., 2008). This reaction requires at least two unpaired nucleotides at the 5′ end, helping to explain the protective effect of the 5′-terminal stem-loop structures that are present on some long-lived transcripts in *E. coli* (Foley et al., 2015). Apart from this strict requirement, *E. coli* RppH is able to remove pyrophosphate from RNAs that begin with any 5′-terminal sequence, although it has a modest preference for A over G at position 1 and for a purine at position 2 (Foley et al., 2015; Vasilyev and Serganov, 2015). The purified enzyme is also able to remove a single phosphate from the 5′ end of diphosphorylated transcripts synthesized *in vitro* (Vasilyev and Serganov, 2015), again by cutting between the α and β phosphates.

RppH plays a crucial role in 5′-end-dependent mRNA degradation in *E. coli*, where deletion of the *rppH* gene reduces the percentage of full-length transcripts that are monophosphorylated almost to zero and prolongs the lifetime of hundreds of mRNAs (Deana et al., 2008) while also impairing the ability of pathogenic *E. coli* to invade human cells (Badger et al., 2000). By contrast, overproducing RppH has little effect on the phosphorylation state or half-life of the mRNAs it targets, suggesting that the rate of formation of the full-length monophosphorylated intermediate may be limited by the cellular concentration of an ancillary factor or by a hypothetical step that precedes attack by RppH (Luciano et al., 2012). This observation led to the discovery that the specific activity of RppH is boosted 2–3 fold in *E. coli* by binding to the diaminopimelate epimerase DapF (Lee et al., 2014). However, the possibility of a prior step that triggers the action of RppH has not previously been explored.

We have now investigated whether conversion of a 5′-terminal triphosphate to a monophosphate in *E. coli* occurs in a single step by pyrophosphate removal, as has commonly been assumed. Our examination of representative triphosphorylated *E. coli* transcripts reveals that they are first transformed into diphosphorylated RNAs, which accumulate to a high cellular concentration, and that the latter RNAs, not their triphosphorylated precursors, are the preferred substrates of RppH. These results indicate that a previously unrecognized event enables 5′-end-dependent mRNA degradation in *E.*

coli and raise the possibility of an important role for diphosphorylated 5′ ends in other RNA-related cellular processes.

RESULTS

Comparative reactivity of diphosphorylated and triphosphorylated RNA as RppH substrates

In principle, the conversion of a 5′-terminal triphosphate to a monophosphate could occur in one step by pyrophosphate removal or in two steps by a mechanism involving sequential loss of the γ and β phosphates and the transient production of a diphosphorylated intermediate. However, whether diphosphorylated RNA molecules exist in bacterial cells has not previously been investigated. To begin to address the possibility of a diphosphorylated intermediate in 5′-end-dependent mRNA degradation in *E. coli*, we first compared the reactivity of diphosphorylated and triphosphorylated RNA as substrates for RppH (Figure 1A). To conduct this test, we used a variant of the *E. coli yeiP* transcript, which encodes a paralog of the translation elongation factor EF-P and decays by an RppH-dependent mechanism *in vivo* (Deana et al., 2008; Richards et al., 2012). This variant (*yeiP*-U2G) contained a U-to-G substitution at the second nucleotide to facilitate its synthesis by T7 RNA polymerase.

Diphosphorylated and triphosphorylated *yeiP*-U2G RNAs were prepared by *in vitro* transcription along with another diphosphorylated transcript that was included as an internal standard in every experiment. The pairwise reaction of these substrates with purified *E. coli* RppH was examined by monitoring the conversion of each to a monophosphorylated product as a function of time. This was accomplished by PABLO, a splinted ligation assay in which the 5′ end of monophosphorylated RNA is joined to a DNA oligonucleotide (Celesnik et al., 2007, 2008). By contrast, diphosphorylated RNA undergoes ligation at a meager rate (Figure S1), and triphosphorylated RNA is completely unreactive (Celesnik et al., 2007). The ligation product and any remaining unligated RNA are then separated by gel electrophoresis and quantified by Northern blotting. Although the ligation reaction is not sufficiently fast to proceed all the way to completion, even with fully monophosphorylated RNA, the percentage of 5′ ends that are monophosphorylated can be accurately calculated from the ratio of the ligation yield for a sample of interest to that of a fully monophosphorylated control sample (Luciano et al., 2012).

Using this procedure, the reactivity of diphosphorylated and triphosphorylated *yeiP*-U2G RNA as substrates of *E. coli* RppH was compared (Figure 1B, C). These rate measurements demonstrated that diphosphorylated *yeiP*-U2G reacts with RppH at least three times faster than its triphosphorylated counterpart, while the reaction rate of the diphosphorylated internal standard did not vary.

Previous studies have demonstrated that the reactivity of triphosphorylated substrates with *E. coli* RppH is influenced by the identity of the nucleotide at the second position, where a purine (especially G) is preferred over a pyrimidine (Foley et al., 2015; Vasilyev and Serganov, 2015). To determine whether this sequence preference also applies to diphosphorylated substrates, we compared the reaction rates of four dinucleotide substrates

(AG, AA, AU, and AC) bearing two or three phosphates at the 5′ end. The progress of each reaction was monitored by using anion-exchange chromatography to separate the substrate and product, which were then detected spectrophotometrically (Figure 2A). In every case, the diphosphorylated substrate reacted with *E. coli* RppH at least ten times faster than its triphosphorylated counterpart (Figure 2B, Table S1). Each substrate yielded a monophosphorylated dinucleotide as the sole reaction product; no diphosphorylated intermediate was detected for the triphosphorylated substrates. Moreover, as previously reported for triphosphorylated RNA, the order of reactivity of the diphosphorylated substrates with RppH was AG ≥ AA > AU ≥ AC.

Assay for detecting diphosphorylated intermediates in cellular RNA

The much greater reactivity of *E. coli* RppH toward diphosphorylated versus triphosphorylated RNA raised the possibility that the former might be its principal biological substrate, a notion consistent with the hypothesis that the conversion of 5′-terminal triphosphates to monophosphates might often proceed via a diphosphorylated intermediate. To ascertain whether such decay intermediates exist in cells, we devised an assay – Phosphorylation Assay by Capping Outcome (PACO) – that makes it possible to determine the percentage of a particular RNA that is diphosphorylated at the 5′ end (Figure 3A). This method is based on the substrate specificity of the RNA guanylyltransferase that catalyzes the second step of RNA capping in eukaryotic cells: the reaction of GTP with a diphosphorylated 5′ end to add an unmethylated cap (Shuman, 2001). We reasoned that such capping would render the 5′ end of diphosphorylated RNA resistant to alkaline phosphatase, whereas the 5′-terminal phosphates of triphosphorylated or monophosphorylated RNA would remain susceptible to removal by alkaline phosphatase due to the inability of the guanylyltransferase to cap those RNAs. Subsequent pyrophosphatase treatment would release the cap from transcripts that had originally been diphosphorylated to produce a monophosphorylated product that could be detected and quantified by PABLO.

The specificity of PACO was tested by using the RNA guanylyltransferase of *Schizosaccharomyces pombe* (Pce1) (Pei and Shuman, 2002) to analyze *in vitro* transcribed *yeiP*- U2G RNA bearing one, two, or three phosphates at the 5′ end (Figure 3B). In each case, the *in vitro* transcript was mixed with total *E. coli* RNA from *ΔyeiP* cells to simulate the conditions of an actual assay of an endogenous *E. coli* transcript. As anticipated, diphosphorylated *yeiP*-U2G was capped and subsequently ligated with a high yield (69%). The failure to achieve a yield of 100% was due primarily to incomplete ligation of the monophosphorylated assay intermediate to the DNA oligonucleotide, as evidenced by the 80% ligation yield observed when all prior steps except pyrophosphatase treatment were omitted from the procedure, but was also due in part to incomplete capping by Pce1. From these values and some other minor corrections (see STAR Methods), we calculated a capping efficiency (E_D) of 0.90 ± 0.06 for the diphosphorylated substrate on a scale from 0 (no capping) to 1 (complete capping) (Tables S2 and S3). Ligation was observed for this substrate only when it was capped by Pce1 prior to being treated with alkaline phosphatase. The triphosphorylated and monophosphorylated RNAs yielded significantly smaller amounts of ligation product in the assay (E_T = 0.31 ± 0.09 and E_M = 0.04 ± 0.03,

respectively). This lack of strict specificity appears to be an intrinsic property of Pce1, as demonstrated by the complete absence of a ligation product when treatment with this enzyme was omitted from the assay, and it is a property shared by other RNA guanylyltransferases (Yu and Shuman, 1996; Chen et al., 1999). These imperfections can all be accommodated when analyzing biological RNA samples, as it is possible to compensate mathematically for both the incomplete reactivity of diphosphorylated RNA and partial reactivity of triphosphorylated and monophosphorylated RNA by using the following equation to calculate the fraction of a particular RNA that is diphosphorylated:

$$D=\frac{(Y/E_L)-E_T\,(1-M)-E_M\,(M)}{E_D-E_T}$$

where D is the diphosphorylated fraction, M is the monophosphorylated fraction (as determined by PABLO), Y is the fractional PACO ligation yield, and E_L is the ligation efficiency of fully monophosphorylated RNA. This equation is derived from two simpler ones: the fraction of RNA that becomes capped (Y/E_L) = E_T T + E_D D + E_M M and T + D + M = 1, where T is the triphosphorylated fraction.

Presence of diphosphorylated RNA in *E. coli*

We next used PACO to investigate whether diphosphorylated RNA could be detected in *E. coli*. If formed, such RNAs might have a fleeting existence *in vivo* due to their susceptibility to rapid phosphate removal by RppH. Therefore, we decided to test for their presence in cells containing or lacking this enzyme. By performing these tests on cellular *yeiP*-U2G mRNA in parallel with the *in vitro* transcribed *yeiP*-U2G standards shown in Figure 3B, whose length and sequence were identical to those of the cellular transcript, it was possible to accurately quantify the fraction of this transcript that was diphosphorylated in *E. coli*.

Diphosphorylated *yeiP*-U2G mRNA was detected at substantial levels in both the presence and absence of RppH. In log-phase *rppH*$^+$ cells, 34 ± 6% of *yeiP*-U2G was diphosphorylated at steady state (Figure 3C, Tables S4 and S5). This value rose to 108 ± 13% in the absence of RppH. No ligation was observed without prior capping by Pce1, evidence that none of the cellular *yeiP*-U2G mRNA was intrinsically resistant to treatment with alkaline phosphatase. Parallel analysis of the same RNA samples by PABLO showed that nearly all the rest of the *yeiP*-U2G mRNA in the *rppH*$^+$ strain was monophosphorylated (71 ± 3%), whereas little or none was monophosphorylated in *ΔrppH* cells (−3 ± 1%) (Figure 3D). Consequently, it appears that almost none of this transcript remained triphosphorylated at steady state in either cell type. We also compared PACO ligation yields for wild-type *yeiP* mRNA in cells containing or lacking RppH. Although the 5′-terminal sequence of this transcript (AU…) prevented its synthesis by T7 RNA polymerase and therefore precluded precise quantitative analysis, a substantial fraction of *yeiP* mRNA appeared to be diphosphorylated in *rppH*$^+$ cells and even more was diphosphorylated in *ΔrppH* cells (Figure S2), results consistent with those for the U2G variant.

To begin to assess how common diphosphorylated mRNAs are in *E. coli*, we also examined the 5′ phosphorylation state of the *metE* transcript, which encodes a homocysteine

transmethylase important for methionine biosynthesis. This message was chosen because its decay rate in *E. coli* is RppH-dependent (Figure S3) and its 5′-terminal nucleotide sequence (GUAAAC…) is completely different from that of *yeiP*-U2G (AGAUUU…). PACO analysis in conjunction with a set of *in vitro* transcribed *metE* standards (Figure 4A), whose length and sequence matched those of the cellular transcript, revealed that 51 ± 8% of *metE* mRNA is diphosphorylated in cells containing RppH, a value that rises to 96 ± 7% in *ΔrppH* cells (Figure 4B, Tables S2–S5). Because 27 ± 2% of *metE* transcripts are monophosphorylated when RppH is present (versus −5 ± 1% in *ΔrppH* cells) (Figure 4C), we calculate that only ~22% of *metE* mRNA is ordinarily triphosphorylated at steady state.

To confirm the presence of diphosphorylated mRNA in *E. coli*, we compared the number of phosphates present in the capped 5′ ends produced by the reaction of Pce1 with either cellular *yeiP*-U2G mRNA or triphosphorylated, diphosphorylated, and monophosphorylated *yeiP*-U2G standards synthesized by *in vitro* transcription. Each was capped by prolonged reaction with Pce1 in the presence of [α-^{32}P]GTP, and the capped 5′-terminal nucleotide was then released from the RNA by hydrolysis with nuclease S1 and examined by thin layer chromatography and autoradiography. As expected, Pce1 reacted with the diphosphorylated standard to generate a capped product whose digestion with S1 released radiolabeled P^1-guanosine-P^3-adenosine-5′,5′-triphosphate (GpppA) (Figure 3E). Capping an equal concentration of the triphosphorylated standard and subsequent hydrolysis produced primarily P^1-guanosine-P^4-adenosine-5′,5′-tetraphosphate (GppppA). Little if any capped reaction product was observed for the monophosphorylated standard. Parallel analysis of *yeiP*-U2G mRNA purified from total RNA that had been extracted from either wild-type or *ΔrppH* cells yielded GpppA as the sole radioactive product of RNA capping, verifying that diphosphorylated mRNA is abundant in *E. coli*. As expected, *yeiP*-U2G from *ΔrppH* cells, where virtually all of that transcript is diphosphorylated, yielded about three times as much GpppA as did a similar amount of the same transcript from wild-type cells, where 71% is monophosphorylated.

Finally, to rule out the possibility that the phosphorylation state of transcripts might be perturbed during RNA extraction from *E. coli*, fully triphosphorylated, diphosphorylated, or monophosphorylated *yeiP*-U2G mRNA that had been synthesized by *in vitro* transcription was added to intact *E. coli* cells lacking a *yeiP* gene, and total RNA was then extracted from those cells. The extraction procedure had no effect on the phosphorylation state of the spiked-in transcripts, as judged by PACO and PABLO (Figure S4).

Competitive 5′-terminal incorporation of ATP versus ADP by *E. coli* RNA polymerase

In principal, the great excess of diphosphorylated *yeiP*-U2G and *metE* mRNA over their triphosphorylated counterparts could be a consequence of the preferential synthesis of diphosphorylated transcripts by RNA polymerase or the swift removal of the γ phosphate of triphosphorylated primary transcripts shortly after they are made. To distinguish between these possibilities, we compared the incorporation of ATP and ADP at the 5′ end of a transcript during its synthesis by purified *E. coli* RNA polymerase. This RNA, EcIVTa, which bore a single, 5′-terminal adenylate nucleotide, was produced by *in vitro* transcription at various ATP : ADP ratios, and its 5′ phosphorylation state was examined by PACO. The

ratio of triphosphorylated to diphosphorylated EcIVTa exceeded the ratio of ATP to ADP present during its synthesis by approximately five-fold (Figure 5). These results indicate that *E. coli* RNA polymerase favors ATP over ADP when initiating transcription. In view of the ratio of nucleotides available for transcription initiation in *E. coli*, which are predominantly triphosphorylated (ATP : ADP : AMP = 92 : 5 : 3 and GTP : GDP : GMP = 87 : 12 : 1 in minimal glucose medium (Bennett et al., 2009)), we conclude that both *yeiP*-U2G and *metE* mRNA are synthesized with a 5′-terminal triphosphate. Evidently, the triphosphate is then rapidly converted to a more stable diphosphate, which eventually undergoes β-phosphate removal by RppH as a prelude to 5′-end-dependent degradation.

Relative reactivity of diphosphorylated RNA as an RNase E substrate

RNase E has a well documented preference for monophosphorylated over triphosphorylated substrates (Mackie, 1998; Jiang et al., 2000; Tock et al., 2000). The long lifetime of the diphosphorylated mRNAs that accumulate in *E. coli* when RppH is absent suggested that they, like their triphosphorylated precursors, are likely to be cleaved slowly by RNase E. To test this hypothesis, we examined the rate at which this enzyme cuts diphosphorylated *yeiP*-U2G RNA, whose the 5′ untranslated region is known to contain several RNase E cleavage sites (Richards et al., 2012; Richards and Belasco, 2016). Purified N-RNase E (the catalytic amino-terminal domain of RNase E) was added to *in vitro* transcribed *yeiP*-U2G RNA bearing one, two, or three phosphates at the 5′ end, and the reaction was monitored by Northern blotting (Figure 6). The monophosphorylated substrate was rapidly cut to produce multiple discrete cleavage products resembling decay intermediates observed *in vivo*. By contrast, the diphosphorylated and triphosphorylated substrates were both cut much more slowly, demonstrating that a 5′-terminal diphosphate is not able to accelerate RNase E cleavage significantly.

DISCUSSION

Until now, it has commonly been assumed that the 5′ ends of bacterial RNAs are ordinarily either triphosphorylated as a result of transcription initiation with a nucleoside triphosphate (Maitra et al., 1965) or monophosphorylated as a consequence of subsequent pyrophosphate removal or RNA cleavage (Crouch, 1974; Kole and Altman, 1981; Szeberényi et al., 1983; Deana et al., 2008), with rare exceptions (Collins et al., 2007; Cook et al., 2013; Cahová et al., 2015). However, direct evidence for triphosphorylated RNA in bacterial cells is rather limited, as it is based largely on the detection of triphosphorylated fragments among the products of chemical or enzymatic digestion of *E. coli* RNA (Jorgensen et al., 1969; Ginsburg and Steitz, 1975; Bieger and Nierlich, 1989). Our finding that diphosphorylated *yeiP*-U2G and *metE* mRNA are each much more abundant than their triphosphorylated counterparts in *E. coli* (34–51% versus only 0–22%) refutes the putative predominance of triphosphorylated mRNA 5′ ends and suggests that the 5′-terminal triphosphate of both primary transcripts is quickly converted to a diphosphate as the initial event in their 5′-end-dependent degradation (Figure 7). This modification creates a better substrate for RppH, which is able to remove the β phosphate from the diphosphorylated species much faster than it could have removed pyrophosphate from the triphosphorylated primary transcript.

Sequential loss of the γ and β phosphates generates a monophosphorylated intermediate susceptible to rapid cleavage by RNase E.

The finding that a substantial fraction of each mRNA tested is diphosphorylated and that this fraction increases to ~100% in the absence of RppH suggests that stepwise conversion of the triphosphorylated primary transcript to a monophosphorylated product vulnerable to ribonuclease attack is the principal mechanism by which 5′-end-dependent RNA degradation is triggered in *E. coli*. This mechanism is also likely to predominate in other proteobacterial species, most of which contain orthologs of *E. coli* RppH (Foley et al., 2015) that are expected to share its preference for diphosphorylated substrates. Nevertheless, it is possible that in some cases γ phosphate removal may be sufficiently slow that RppH converts triphosphorylated 5′ ends to monophosphates in a single step without waiting for the γ phosphate to be removed.

Previously, the presence and functional significance of diphosphorylated 5′ ends had gone unrecognized due to the lack of an analytical method for distinguishing such ends from their triphosphorylated counterparts. To detect and quantify diphosphorylated mRNA in *E. coli*, we devised a novel assay (PACO) that is based on the specificity of the RNA guanylyltransferase important for mRNA capping in eukaryotic nuclei. Key to the utility of PACO is the quantitative nature of this assay, which makes it possible not only to detect diphosphorylated RNAs but also to determine their relative abundance. Like other enzymes of its kind (Yu and Shuman, 1996; Chen et al., 1999), the RNA guanylyltransferase employed in these assays (Pce1 of *Schizosaccharomyces pombe*) is not entirely specific for diphosphorylated RNA, making it impractical to drive the capping reaction to completion by using an excess of this enzyme. Instead, it was necessary to interrupt the reaction just as the capping of diphosphorylated RNA was nearing completion and to compare the reaction yield for cellular RNA to that for a set of triphosphorylated, diphosphorylated, monophosphorylated standards that had been synthesized by *in vitro* transcription and were identical in sequence and length to the cellular transcript under investigation. This knowledge, together with an independent measurement of the percentage of the cellular transcript that is monophosphorylated, provided all the information required to calculate how much of that transcript is diphosphorylated *in vivo*. The fact that no PACO ligation was observed without prior capping by Pce1, i.e. that none of the cellular *yeiP*-U2G or *metE* mRNA was intrinsically resistant to alkaline phosphatase, indicates that neither 5′ end is protected detectably by a cap-like structure, a finding consistent with previous evidence (Cahová et al., 2015). Though effective for determining the phosphorylation state of individual RNAs, PACO is not suitable for examining an entire transcriptome because the assay must be calibrated with a distinct set of cognate standards and a PABLO measurement for each transcript under investigation.

Our finding that the diphosphorylated and monophosphorylated forms of *yeiP*-U2G and *metE* together account for ~80–100% of each full-length transcript means that little triphosphorylated RNA remains for either of them. The great excess of diphosphorylated over triphosphorylated 5′ ends stands in stark contrast to the ratio of nucleotides available for transcription initiation in *E. coli*, which are predominantly triphosphorylated. Moreover, our data indicate that *E. coli* RNA polymerase preferentially incorporates NTPs rather than

NDPs at the 5′ end of transcripts. Therefore, it appears that *E. coli* cells contain one or more enzymes that can rapidly remove the γ phosphate from primary transcripts. RppH does not appear to be the source of this triphosphatase activity, as no diphosphorylated intermediate was detected *in vitro* during the conversion of triphosphorylated 5′ ends to monophosphorylated 5′ ends by the purified *E. coli* enzyme (Figure 2A), a reaction in which pyrophosphate, not orthophosphate, is the principal by-product (Deana et al., 2008). Furthermore, contrary to the phenotype expected for a triphosphatase-deficient mutant, deleting the *rppH* gene does not diminish the abundance of diphosphorylated 5′ ends in *E. coli* (Figures 3C and 4B). For similar reasons (Lee et al., 2014 and PACO analysis of RNA from *ΔdapF* cells [data not shown]), it is also unlikely that DapF, which forms a complex with RppH, functions as an RNA triphosphatase in *E. coli*. Nor does *E. coli* contain a homolog of the eukaryotic RNA triphosphatases that catalyze the first step in RNA capping. Whatever the source of this activity may be, it apparently can act on RNAs with a variety of 5′-terminal sequences, including those that begin with either A or G. Nevertheless, it appears to favor the former, as judged from the markedly greater steady-state ratio of diphosphorylated to triphosphorylated *yeiP*-U2G versus *metE* mRNA despite the likely preference of RppH for the first two nucleotides of *yeiP*-U2G (AG versus GU (Foley et al., 2015; Vasilyev and Serganov, 2015)).

Irrespective of its 5′-terminal sequence, the diphosphorylated RNA generated by the putative RNA triphosphatase is a much better substrate for RppH than its triphosphorylated precursor. The ≥3–10-fold greater reactivity of diphosphorylated RNA explains the need for γphosphate removal despite the ability of *E. coli* RppH to convert 5′-terminal triphosphates directly to monophosphates. The basis for the faster reaction rate of diphosphorylated substrates is not apparent from the published structures of the liganded enzyme (Vasilyev and Serganov, 2015) or the relevant pK_a of the leaving group, which is significantly higher for phosphate than for pyrophosphate (12.4 versus 9.3).

RNA modifications that previously went undetected are now known to play major roles in governing gene expression in both prokaryotic and eukaryotic organisms (Deana et al., 2008; Schwartz, 2016). For instance, recent studies have shown that adenosine methylation can stimulate translation and accelerate mRNA degradation in human cells (Wang et al., 2014; Wang et al., 2015; Meyer et al., 2015). The discovery that the formation of diphosphorylated RNA enables 5′-end-dependent degradation in *E. coli* provides a prime example of such a phenomenon in bacteria and a key insight into the mechanism of an important regulatory pathway that has been implicated in microbial pathogenesis. Nevertheless, it seems unlikely that bacteria evolved the ability to produce diphosphorylated RNA solely as a mechanism for initiating degradation, as RppH alone is able to convert 5′-terminal triphosphates directly to monophosphates, albeit more slowly than it acts on diphosphates. Instead, the remarkable abundance of diphosphorylated RNA in *E. coli* raises the possibility that this novel phosphorylation state may govern additional RNA-dependent processes, perhaps by enabling binding by regulatory proteins other than RppH or by preventing RNA 5′ ends from being mistaken for nucleoside triphosphates. However diverse its biological functions might be, the discovery of diphosphorylated RNA in *E. coli* demonstrates that modifying the phosphorylation state of bacterial mRNAs is a more

complex process than previously realized and suggests that the 5′ end of bacterial transcripts may be a busier and more influential locale than heretofore imagined.

STAR METHODS

CONTACT FOR REAGENT AND RESOURCE SHARING

Further information and requests for resources and reagents should be directed to and will be fulfilled by the lead contact, Joel G. Belasco (joel.belasco@med.nyu.edu).

EXPERIMENTAL MODEL AND SUBJECT DETAILS

Growing cells for RNA extraction—Saturated cultures of *E. coli* grown in MOPS-glucose (Neidhardt et al., 1974) were diluted into fresh MOPS-glucose (without antibiotic) to an initial OD_{650} of less than 0.01 and shaken at 37ºC until the OD_{650} reached 0.28–0.32.

METHOD DETAILS

Strains and plasmids—Measurements of the 5′ phosphorylation state and half-life of mRNA were performed in the *E. coli* K-12 strain BW25113 (Datsenko and Wanner, 2000) and an isogenic derivative thereof bearing an in-frame deletion of the *rppH* coding region. In addition, the strains used to analyze *yeiP* and *yeiP*-U2G mRNA lacked the chromosomal copy of the *yeiP* gene and instead contained a plasmid (pYeiP1 or pYeiP1-U2G, respectively (Richards et al., 2012; Foley et al., 2015)) encoding the transcript of interest. Each chromosomal deletion mutant was constructed by P1 transduction of BW25113 with the corresponding *kan*-disrupted gene from the Keio collection (Baba et al., 2006) followed by excision of the *kan* gene.

Protein purification—*E. coli* RppH bearing an amino-terminal hexahistidine tag (MHHHHHHG) was produced in *E. coli* from plasmid pPlacRppH6, purified by affinity chromatography on TALON beads (Clontech), and stored at −80°C in a buffer containing 10 mM HEPES (pH 7.5), 0.3 M NaCl, and 50% (v/v) glycerol (Foley et al., 2015; Vasilyev and Serganov, 2015). *E. coli* DapF bearing six additional residues (SGSGSG) at the amino terminus was generated from a protein fusion in which hexahistidine and SUMO tags were joined in tandem to the amino terminus of DapF. This protein fusion was produced in *E. coli* from plasmid pSumo-DapF and purified from cell extracts by affinity chromatography on a HisTrap column (GE Healthcare). The tags were removed by cleavage with hexahistidine-tagged ULP1 protease, and the flow-through from a second HisTrap column (no imidazole) was then concentrated and further fractionated by gel filtration through Superdex 200 (GE Healthcare). The purified DapF was stored at −80°C in a buffer containing 20 mM Tris-HCl (pH 8.0), 0.25 M NaCl, and 1 mM dithiothreitol. ULP1 bearing an amino-terminal hexahistidine tag was produced in *E. coli* from plasmid pET28b-ULP1 (Mossessova and Lima, 2000), purified from cell extracts by affinity chromatography on a HisTrap column (GE Healthcare), concentrated/exchanged into a buffer containing 20 mM Tris-HCl (pH 8.0), 500 mM NaCl, 1 mM EDTA, and 0.05% 2-mercaptoethanol, and stored at −80°C.

Schizosaccharomyces pombe Pce1 bearing an amino-terminal His_6Smt3 domain was produced in *E. coli* from plasmid pSMT3-Pce1, which was a generous gift from Christopher

Lima (Memorial Sloan Kettering Cancer Center, New York) (Doamekpor et al., 2014), purified from cell extracts by elution from TALON beads (Clontech), concentrated/exchanged into a buffer containing 20 mM Tris-HCl (pH 8.0), 50 mM NaCl, 1 mM 2-mercaptoethanol, and 20% (v/v) glycerol, and stored at −20°C.

T4 DNA ligase bearing an amino-terminal hexahistidine tag was produced from plasmid pPlacT4L in the RNase H-deficient *E. coli* strain MIC2067 (Itaya et al., 1999) and then purified from cell extracts by elution from TALON beads (Clontech) followed by anion-exchange chromatography on an UNO Q1 column (Bio-Rad). The purified protein was concentrated/exchanged into a buffer containing 10 mM Tris-HCl (pH 7.4), 50 mM KCl, 0.1 mM EDTA, 1 mM dithiothreitol, and 50% (v/v) glycerol and stored at −80°C.

E. coli RNA polymerase holoenzyme containing σ^{70} was provided by Vitaly Epshtein and Evgeny Nudler (NYU School of Medicine, New York) (Nudler et al., 2003).

N-RNase E comprised amino acid residues 1-529 of *E. coli* RNase E joined to a carboxy-terminal extension containing hexahistidine and Myc-epitope tags (GGAAAHHHHHHVAAEQKLISEEDLNGAARSA). It was produced from plasmid pNRNE7529 in *E. coli*, purified from cell extracts by elution from TALON beads (Clontech), concentrated/exchanged into a buffer containing 20 mM Tris-HCl (pH 7.5), 0.5 M NaCl, 10 mM dithiothreitol, and 20% (v/v) glycerol, and stored at −80°C (Richards and Belasco, 2016).

RNA synthesis by *in vitro* transcription—Triphosphorylated *yeiP*-U2G and *metE* RNA was synthesized *in vitro* by using T7 RNA polymerase to transcribe a PCR-amplified DNA template containing a T7 ϕ2.5 (*yeiP*-U2G) or ϕ6.5 (*metE*) promoter in the presence of ATP, GTP, CTP, and UTP. Their diphosphorylated and monophosphorylated counterparts were synthesized in the presence of an 18–30 fold molar excess of ADP (4.4 mM) or AMP (7.5 mM) over ATP (0.25 mM) in the case of *yeiP*-U2G or of GDP (7.5 mM) or GMP (7.5 mM) over GTP (0.25 mM) in the case of *metE*. These *in vitro* transcripts were identical to the corresponding cellular transcripts in their entirety (*yeiP*-U2G: 654 nt in length; *metE*: 2,464 nt in length). In addition, a diphosphorylated RNA (*yeiP*-std128) comprising the first 128 nucleotides of *yeiP*-U2G except for a GGU → CCC substitution at positions 68–70 was prepared by *in vitro* transcription for use as an internal standard in rate measurements with purified RppH. For details about nucleotide purity and oligonucleotide primers, see Tables S6 and S7.

Reactivity of RppH with polynucleotides—Either diphosphorylated or triphosphorylated *yeiP*-U2G RNA (1 pmol) was combined with a diphosphorylated internal standard (1 pmol of *yeiP*-std128, a *yeiP*-U2G variant resistant to cleavage by the 10–23 DNAzyme DZyeiP69) in a total volume of 50 μl. A 5-μl sample was removed as the 0-min timepoint, and another 5-μl sample was removed and processed as a ligation control by exhaustive treatment with excess RppH (200 nM at 37°C for 2 hr). The remainder (40 μl) was prewarmed to 37°C and combined with prewarmed RppH (40 μl) to initiate the reaction. The final reaction mixture (80 μl) contained the following: diphosphorylated or triphosphorylated *yeiP*-U2G RNA (10 nM), diphosphorylated internal standard RNA (10

nM), HEPES, pH 7.5 (20 mM), $MgCl_2$ (10 mM), dithiothreitol (1 mM), glycerol (1%), rRNasin (2 units/μl; Promega), RppH (5 nM), and DapF (10 nM). To monitor the progress of the reaction, samples (10 μl) were removed at time intervals, quenched with excess EDTA, phenol extracted, and ethanol precipitated. Each sample was then examined by PABLO in conjunction with the selective cleavage of *yeiP*-U2G RNA and its ligation product by DZyeiP69 to increase their electrophoretic mobility. The extent of conversion of diphosphates or triphosphates to monophosphates at each timepoint was calculated by normalizing the measured ligation yield to that of the fully monophosphorylated ligation control.

Reactivity of RppH with dinucleotides—Dinucleotide substrates bearing a 5′-terminal diphosphate or triphosphate were prepared by *in vitro* transcription with T7 RNA polymerase (Vasilyev and Serganov, 2015; Vasilyev and Serganov, 2016). To measure RppH activity, reaction mixtures containing 50 mM HEPES, pH 7.5, 10 mM $MgCl_2$, 0.1% Triton X-100, 100 μM di- or triphosphorylated dinucleotide, and 100 nM RppH were incubated at 37°C for 0–10 min, and 50-μl samples taken at time intervals were quenched by dilution with 50 mM sodium acetate, pH 5.0 (500 μl). The substrate and product in each sample were separated by anion-exchange chromatography on a 5×50 mm Mono Q column by applying a gradient of 0–0.5 M NaCl in 10 mM Tris-HCl, pH 8.0, while recording the elution profile spectrophotometrically at 260 nm. Peak areas corresponding to the substrate and product were integrated using UNICORN software (GE Healthcare). Each reaction was repeated two times.

RNA extraction from *E. coli*—Total cellular RNA was extracted from *E. coli* cultures that had been grown to mid-log phase at 37°C in MOPS-glucose medium. A culture sample (10–15 ml) was rapidly chilled by pipetting it into a 50-ml centrifuge tube filled with crushed ice, and the bacteria were pelleted by centrifugation at 6,000 × *g* for 10 min at 0°C. The cell pellet was resuspended at 0°C in 125 μl of ice-cold buffer A (0.3 M sucrose, 10 mM sodium acetate, pH 4.5, 10 mM EDTA), transferred to a chilled microfuge tube, mixed with 250 μl of room-temperature buffer B (2% SDS, 10 mM sodium acetate, pH 4.5), and heated to 75°C for 3 min to lyse the cells. The cell lysate was extracted three times with 250 μl of hot, unneutralized, water-saturated phenol by vigorously agitating the mixture and then heating it to 75°C for 3 min. After each phenol extraction, the mixture was chilled rapidly in a dry ice/ethanol bath and then centrifuged at 21,000 × *g* for 5 min before transferring the aqueous layer to a new microfuge tube. Finally, the RNA was precipitated by mixing the aqueous layer of the last phenol extraction (up to 450 μl) with 3 M sodium acetate, pH 4.8 (45 μl) and ethanol (1 ml), cooled to −20°C for 30 min, pelleted by centrifugation at 21,000 × *g* for 15 min, washed with 70% ethanol, air-dried, dissolved in water (30–70 μl) to a concentration of 0.5–2.0 μg/μl, and stored at −20°C.

PABLO—To determine the percentage of a particular *E. coli* transcript that was monophosphorylated, total cellular RNA was combined with oligonucleotide X (0.44 μM), oligonucleotide Y (0.09 μM), and a transcript-specific 10–23 DNAzyme (8.9 μM) (see Table S7) in a total volume of 45 μl, heated to 85°C for 5 min, slowly cooled to 30°C, and then placed on ice for at least 2 min. A solution (35 μl) containing Tris-HCl, pH 7.5 (114 mM),

$MgCl_2$ (23 mM), dithiothreitol (23 mM), ATP (2.7 mM), rRNasin (1 unit/μl; Promega), and T4 DNA ligase (1.3 μM) was added, and ligation was allowed to proceed for 2 or 4 hr at 37°C before being quenched with EDTA (150 μl of an 8.3 mM solution). The reaction products were phenol extracted, ethanol precipitated, separated by electrophoresis on a 5–6% polyacrylamide-urea gel, and transferred to a Hybond-XL membrane (GE Healthcare) by electroblotting. The blot was then UV-crosslinked and probed with a 5′-radiolabeled oligonucleotide complementary to the RNA of interest. Bands were visualized on a Typhoon Trio imager (GE Healthcare) and quantified by using ImageQuant TL software. As a ligation control, fully monophosphorylated RNA generated by prior treatment with excess RppH (200 nM for 2 hr at 37°C) was analyzed in parallel. When testing reactivity with RppH *in vitro*, the PABLO reactions were performed as above but with four times as much oligo X (1.8 μM), oligo Y (0.36 μM), and 10–23 DNAzyme (35.6 μM) in a total volume of 45 μl.

PACO—To determine the percentage of a particular *E. coli* transcript that was diphosphorylated, total cellular RNA (10 μl, prewarmed) was combined with Pce1 (10 μl, prewarmed) in a reaction mixture containing RNA (5 μg), Tris-HCl, pH 7.5 (50 mM), dithiothreitol (5 mM), GTP (1 mM), $MgCl_2$ (1 mM), rRNasin (2 units/μl; Promega), and Pce1 (100 nM). In parallel, triphosphorylated, diphosphorylated, and monophosphorylated RNAs identical to the entire *E. coli* transcript of interest were synthesized by *in vitro* transcription, added to total RNA (5 μg) from *E. coli* cells devoid of that transcript, and treated identically. The capping reaction was allowed to proceed for 4 min at 37°C before being quenched with EDTA (195 μl of a 4 mM solution), and the reaction products were phenol extracted and ethanol precipitated. The 5′-terminal phosphates of uncapped RNA were next removed by treatment with calf intestine alkaline phosphatase (0.5 units/μl; New England Biolabs) in Tris-HCl, pH 7.9 (100 mM), NaCl (100 mM), $MgCl_2$ (10 mM), dithiothreitol (1 mM), and rRNasin (2 units/μl; Promega) for 1 hr at 37°C, and the reaction products were again phenol extracted and ethanol precipitated. Subsequent treatment of the capped 5’ ends with excess RppH (200 nM for 2 hr at 37°C) converted them all to monophosphates, which were then detected by PABLO in conjunction with DNAzyme cleavage. As a ligation control, fully monophosphorylated RNA generated by prior treatment with excess RppH (200 nM for 2 hr at 37°C) was analyzed in parallel.

Characterization of caps added by Pce1—Total RNA (260 μg) extracted from *E. coli* cells that lacked the chromosomal *yeiP* gene and instead contained plasmid pYeiP1-U2G was fractionated by electrophoresis on a 4.5% polyacrylamide/7 M urea gel. A gel slice containing full-length *yeiP*-U2G mRNA was excised, crushed, and soaked overnight in EDTA (1 mM, pH 8.0), and the extracted RNA was ethanol precipitated. To selectively reduce the length of *yeiP*-U2G mRNA relative to other, co-purified RNAs of a similar size, it was then cleaved 444 nucleotides from the 5′ end by treatment with DZyeiP444 (20 μM) in Tris-HCl, pH 7.5 (50 mM), $MgCl_2$ (10 mM), and dithiothreitol (10 mM) for 4 hr at 37°C. The cleavage products were separated by electrophoresis on a 4.5% polyacrylamide/7 M urea gel, and the fragment comprising the 5′-terminal 444 nucleotides of *yeiP*-U2G mRNA was recovered as described above. In addition, triphosphorylated, diphosphorylated, and monophosphorylated standards identical to the 5′-terminal 444 nucleotides of *yeiP*-U2G mRNA were synthesized *in vitro* by run-off transcription with T7 RNA polymerase. Each

RNA was dissolved in 20 μl of a buffer containing Tris-HCl, pH 7.5 (50 mM), dithiothreitol (5 mM), [α-^{32}P] GTP (0.65 μCi, 0.078 μM), $MgCl_2$ (1 mM), and rRNasin (2 units/μl; Promega) and capped with Pce1 (3.5 μM) for 2 hr at 37°C. The capping reaction was quenched with EDTA (180 μl of a 4.2 mM solution), and the reaction products were phenol extracted and ethanol precipitated. The capped 5′-terminal nucleotide was then released by RNA digestion with S1 nuclease (50 units; Thermo Fisher Scientific) for 30 min at 37°C in 9 μl of a buffer containing sodium acetate, pH 4.5 (40 mM), NaCl (300 mM), and $ZnSO_4$ (2 mM), and the remaining unreacted [α-^{32}P] GTP was hydrolyzed to guanosine and orthophosphate by treatment with calf intestinal alkaline phosphatase (1 unit/μl; New England Biolabs) for 30 min at 37°C in a buffer containing Tris-HCl, pH 8.0 (50 mM) and $MgCl_2$ (10 mM). Finally, the products were analyzed by thin layer chromatography beside GpppA (1 nmol; New England Biolabs) and GppppA (1 nmol; Jena Bioscience) markers on a fluorescent PEI-cellulose plate (J.T. Baker) developed with ammonium sulfate (0.4 M, pH 5.5). The radiolabeled products were detected with a Typhoon Trio imager (GE Healthcare), and the unlabeled GpppA and GppppA markers were detected by UV shadowing.

5′-terminal nucleotide incorporation by *E. coli* RNA polymerase—EcIVTa RNA was synthesized *in vitro* by run-off transcription with *E. coli* RNA polymerase of a 174-bp DNA template that contained a σ^{70} promoter (CTTAAGGTTAACCACCGAATTCATGAGCGCGCACAGTACCACCTTTTTTGCACCA GCAAAAGTGCGAATACCACTTGACAGAAAGGCCCGTCGCGAGTACTTTGTCGCG ATCTTTCTCTGTTGTTCTTCTGTTGGTCTTTTTCCCTGCCCTGTGCGGTCGGCGTT GCGTTCGGT, where the region encoding RNA is underlined). Purified *E. coli* RNA polymerase holoenzyme (16 pmol) was combined with the purified DNA template (8 pmol) in buffer TB50 (40 mM Tris-HCl, pH 8.0, 50 mM NaCl, 10 mM $MgCl_2$) containing GTP (0.1 mM), CTP (0.1 mM), UTP (0.1 mM), and a mixture of ATP and ADP at various molar ratios (2.0 + 0.0 mM, 1.8 + 0.2 mM, 1.0 + 1.0 mM, 0.2 + 1.8 mM, or 0.0 + 2.0 mM). After 1 hr at 37°C, each reaction was quenched with an equal volume of stop solution (20 mM EDTA, 7 M urea), phenol extracted, and ethanol precipitated. The reaction products were then combined with total *E. coli* RNA (5 μg), cleaved 54 nt from the 5′ end by treatment with the 10–23 DNAzyme DZEcIVTa54 (11 μM; see Table S7) for 2 hr at 37°C in a buffer containing Tris-HCl, pH 7.5 (50 mM), $MgCl_2$ (10 mM), and dithiothreitol (10 mM), and analyzed by PACO to determine the ratio of 5′-terminal ADP versus ATP incorporation.

RNA cleavage by purified N-RNase E—Monophosphorylated, diphosphorylated, and triphosphorylated *in vitro* transcripts comprising the first 80 nucleotides of *yeiP*-U2G RNA (37 nM) were digested with purified N-RNase E (175 nM enzyme subunits) at 30°C in a buffer containing 25 mM Bis-tris propane (pH 8.0), 100 mM NaCl, and 15 mM $MgCl_2$. Reaction samples (0.33 pmol) were quenched with excess EDTA at time intervals. These samples were then mixed with total RNA (7.5 μg) from *E. coli* strain BW25113 *ΔyeiP* to facilitate precipitation, ethanol precipitated, subjected to electrophoresis on a 7.5% polyacrylamide-urea gel, and transferred to a Hybond-XL membrane (GE Healthcare) by electroblotting. The blot was UV-crosslinked and probed with a 5′-radiolabeled oligonucleotide (yeiP 80 rev) complementary to the 3′ end of the RNA. Bands were

visualized on a Typhoon Trio imager (GE Healthcare) and quantified by using ImageQuant TL software.

Decay rate of *metE* mRNA in *E. coli*—At time intervals after inhibiting transcription with rifampicin (200 μg/ml), total RNA was extracted from isogenic *E. coli* strains containing or lacking RppH, and the half-life of the *metE* transcript was determined by quantitative RT-PCR analysis with SuperScript III reverse transcriptase (Thermo Fisher Scientific), FastStart Universal SYBR Green Master (Rox) (Roche), and primers specific for *metE* mRNA and 16S rRNA (see Table S7). The initial concentration of the two cDNAs in each sample was determined by fitting the qPCR data to a two-parameter MAK2 model (Boggy and Woolf, 2010; Ritz and Spiess, 2008; Luciano et al., 2012).

QUANTIFICATION AND STATISTICAL ANALYSIS

Quantification—Northern blot band intensities were quantified by using ImageQuant TL software (GE Healthcare). Peak areas for the substrates and products of the reaction of dinucleotides with RppH were determined by using UNICORN software (GE Healthcare).

Statistical analysis—Mean values and standard deviations are provided in Figures 6 and S3 and in the legends of Figures 1 and 5. Standard deviations of the data plotted in Figure 2 are listed in Table S1. Statistical analysis of the 5′ phosphorylation data shown in Figures 3 and 4 is presented in Tables S2, S3, S4, and S5.

Calculating capping efficiencies and phosphorylation states—The capping efficiency for each standard was calculated by using the following set of equations:

$$E_T = \frac{Y_{TS}}{E_{LS}}$$
$$E_D = \frac{(Y_{DS}/E_{LS}) - (Y_{TS}/E_{LS})(1 - D_S)}{D_S}$$
$$E_M = \frac{(Y_{MS}/E_{LS}) - (Y_{TS}/E_{LS})(1 - M_S)}{M_S}$$

where E_T, E_D, and E_M are the capping efficiencies of the triphosphorylated, diphosphorylated, and monophosphorylated standards, respectively. Y_{TS}, Y_{DS}, and Y_{MS} are the fractional PACO ligation yields obtained for each standard, D_S and M_S are the fraction of those standards that are diphosphorylated or monophosphorylated, as calculated from the molar ratio of NDP or NMP to the corresponding NTP during their synthesis by *in vitro* transcription, and E_{LS} is the ligation efficiency of the fully monophosphorylated transcript. (Note that $D_S = M_S = 0$ for the *in vitro* transcribed triphosphorylated standards, $M_S = 0$ for the *in vitro* transcribed diphosphorylated standards, and $D_S = 0$ for the *in vitro* transcribed monophosphorylated standards and that the correction factors $(Y_{TS}/E_{LS})(1 - D_S)$ and $(Y_{TS}/E_{LS})(1 - M_S)$ are very small: 0.005 to 0.021 and 0.005 to 0.007, respectively, depending on the RNA.) These equations were derived from two simpler equations: $(Y_S/E_{LS}) = E_T(T_S) + E_D(D_S) + E_M(M_S)$ and $T_S + D_S + M_S = 1$, where Y_S is the fractional PACO ligation yield for a given standard and T_S is the fraction of a particular standard that is triphosphorylated. Mean values and standard deviations were calculated for Y_{TS}, Y_{DS}, Y_{MS}, and E_{LS} from multiple measurements of each (Table S2) and subsequently used to generate

random Gaussian sample sets of 100,000 values for each of these variables. E_T, E_D, and E_M and their errors were then calculated by Monte Carlo simulation (ciCalc). For each simulation, a histogram was constructed and fit to a spline function, and the mode (peak value) was determined. Because of the asymmetry of the distribution, an error equivalent to one standard deviation was then calculated by integrating outward from the mode until a confidence level of 68.3%, equivalent to one standard deviation, was attained. The modes and errors are reported in Table S3.

The distributions of E_T, E_D, and E_M were then combined with data from PACO and PABLO analysis of cellular RNA to calculate the fraction of diphosphorylated and monophosphorylated *yeiP*-U2G and *metE* mRNA in *E. coli* by Monte Carlo simulation (ciCalc) with the following equations:

$$D = \frac{(Y_D/E_{LD}) - E_T\,(1-M) - E_M\,(M)}{E_D - E_T}$$

$$M = \frac{Y_M - E_{PD}\,(D)}{E_{LM}}$$

where D is the diphosphorylated fraction, M is the monophosphorylated fraction, Y_D and Y_M are the fractional PACO and PABLO ligation yields, E_{LD} and E_{LM} are the ligation efficiencies of fully monophosphorylated RNA in PACO and PABLO experiments, and E_{PD} is the small fraction of diphosphorylated RNA (0.045 for *yeiP*-U2G and 0.075 for *metE* (see Figure S1)) that undergoes ligation by T4 DNA ligase during PABLO. (Note that the correction factors E_M (M) and E_{PD} (D) are very small: −0.002 to 0.030 and 0.015 to 0.073, respectively, depending on the RNA and host genotype.) Random Gaussian sample sets (100,000 values each) were generated from the means and standard deviations of Y_D, E_{LD}, Y_M, and E_{LM} (Table S4) and then used to calculate D and M by iterative Monte Carlo simulation. For an initial estimate of D and its error, we performed a Monte Carlo simulation in which Y_M/E_{LM} was used as an approximation of M. The resulting distribution of values for D and the complete equation for M were then used in a Monte Carlo simulation to calculate M more accurately. This distribution of M values was subsequently used to recalculate D, and so on. After three iterations, the modes of the distributions for D and M had each achieved convergence. These modes and their associated errors (confidence level of 68.3%, equivalent to one standard deviation) are reported in Table S5.

DATA AND SOFTWARE AVAILABILITY

ciCalc: https://www.dropbox.com/sh/tnmfozrubycxq56/AABDh2ex_wfMQ6204byQsYKXa?dl=0 ciCalc computes modes (peak values) and confidence intervals for variables of interest by the Monte Carlo method. These variables are defined by the user as arbitrary functions of other, input variables, which are assumed to have Gaussian distributions with known means and standard deviations that are entered by the user.

Supplementary Material

Refer to Web version on PubMed Central for supplementary material.

Acknowledgments

We are grateful to Patricia Foley, Ang Gao, Vitaly Epshtein, and Evgeny Nudler for providing purified enzymes and to Kevin Belasco and Sisi Ma for help with statistical analysis. This research was supported by fellowships to D.J.L. from the National Institutes of Health (T32AI007180) and the Vilcek endowment and by grants to J.G.B. (R01GM035769) and A.S. (R01GM112940) from the National Institutes of Health.

References

Baba T, Ara T, Hasegawa M, Takai Y, Okumura Y, Baba M, Datsenko KA, Tomita M, Wanner BL, Mori H. Construction of *Escherichia coli* K-12 in-frame, single-gene knockout mutants: the Keio collection. Mol Syst Biol. 2006; 2:2006. 0008.

Badger JL, Wass CA, Kim KS. Identification of *Escherichia coli* K1 genes contributing to human brain microvascular endothelial cell invasion by differential fluorescence induction. Mol Microbiol. 2000; 36:174–182. [PubMed: 10760174]

Bennett BD, Kimball EH, Gao M, Osterhout R, Van Dien SJ, Rabinowitz JD. Absolute metabolite concentrations and implied enzyme active site occupancy in Escherichia coli. Nat Chem Biol. 2009; 5:593–599. [PubMed: 19561621]

Bieger CD, Nierlich DP. Distribution of 5′-triphosphate termini on the mRNA of *Escherichia coli*. J Bacteriol. 1989; 171:141–147. [PubMed: 2464575]

Boggy GJ, Woolf PJ. A mechanistic model of PCR for accurate quantification of quantitative PCR data. PLoS One. 2010; 5:e12355. [PubMed: 20814578]

Cahová H, Winz ML, Höfer K, Nübel G, Jäschke A. NAD captureSeq indicates NAD as a bacterial cap for a subset of regulatory RNAs. Nature. 2015; 519:374–377. [PubMed: 25533955]

Celesnik H, Deana A, Belasco JG. Initiation of RNA decay in *Escherichia coli* by 5′ pyrophosphate removal. Mol Cell. 2007; 27:79–90. [PubMed: 17612492]

Celesnik H, Deana A, Belasco JG. PABLO analysis of RNA: 5′-phosphorylation state and 5′-end mapping. Methods Enzymol. 2008; 447:83–98. [PubMed: 19161839]

Chao Y, Li L, Girodat D, Förstner KU, Said N, Corcoran C, Śmiga M, Papenfort K, Reinhardt R, Wieden HJ, et al. In vivo cleavage map illuminates the central role of RNase E in coding and non-coding RNA pathways. Mol Cell. 2017; 65:39–51. [PubMed: 28061332]

Chen D, Luongo CL, Nibert ML, Patton JT. Rotavirus open cores catalyze 5′-capping and methylation of exogenous RNA: evidence that VP3 is a methyltransferase. Virology. 1999; 265:120–130. [PubMed: 10603323]

Collins JA, Irnov I, Baker S, Winkler WC. Mechanism of mRNA destabilization by the *glmS* ribozyme. Genes Dev. 2007; 21:3356–3368. [PubMed: 18079181]

Cook GM, Robson JR, Frampton RA, McKenzie J, Przybilski R, Fineran PC, Arcus VL. Ribonucleases in bacterial toxin-antitoxin systems. Biochim Biophys Acta. 2013; 1829:523–531. [PubMed: 23454553]

Crouch RJ. Ribonuclease III does not degrade deoxyribonucleic acid-ribonucleic acid hybrids. J Biol Chem. 1974; 249:1314–1316. [PubMed: 4592261]

Datsenko KA, Wanner BL. One-step inactivation of chromosomal genes in *Escherichia coli* K-12 using PCR products. Proc Natl Acad Sci USA. 2000; 97:6640–6645. [PubMed: 10829079]

Deana A, Celesnik H, Belasco JG. The bacterial enzyme RppH triggers messenger RNA degradation by 5′ pyrophosphate removal. Nature. 2008; 451:355–358. [PubMed: 18202662]

Del Campo C, Bartholomäus A, Fedyunin I, Ignatova Z. Secondary structure across the bacterial transcriptome reveals versatile roles in mRNA regulation and function. PLoS Genet. 2015; 11:e1005613. [PubMed: 26495981]

Doamekpor SK, Sanchez AM, Schwer B, Shuman S, Lima CD. How an mRNA capping enzyme reads distinct RNA polymerase II and Spt5 CTD phosphorylation codes. Genes Dev. 2014; 28:1323–1336. [PubMed: 24939935]

Foley PL, Hsieh PK, Luciano DJ, Belasco JG. Specificity and evolutionary conservation of the *Escherichia coli* RNA pyrophosphohydrolase RppH. J Biol Chem. 2015; 290:9478–9486. [PubMed: 25657006]

Garneau NL, Wilusz J, Wilusz CJ. The highways and byways of mRNA decay. Nat Rev Mol Cell Biol. 2007; 8:113–126. [PubMed: 17245413]

Ginsburg D, Steitz JA. The 30 S ribosomal precursor RNA from *Escherichia coli*. A primary transcript containing 23 S, 16 S, and 5 S sequences. J Biol Chem. 1975; 250:5647–5654. [PubMed: 1095585]

Hui MP, Foley PL, Belasco JG. Messenger RNA degradation in bacterial cells. Annu Rev Genet. 2014; 48:537–559. [PubMed: 25292357]

Itaya M, Omori A, Kanaya S, Crouch RJ, Tanaka T, Kondo K. Isolation of RNase H genes that are essential for growth of *Bacillus subtilis* 168. Journal of bacteriology. 1999; 181:2118–2123. [PubMed: 10094689]

Jiang X, Diwa A, Belasco JG. Regions of RNase E important for 5′-end-dependent RNA cleavage and autoregulated synthesis. J Bacteriol. 2000; 182:2468–2475. [PubMed: 10762247]

Jorgensen SE, Buch LB, Nierlich DP. Nucleoside triphosphate termini from RNA synthesized in vivo by *Escherichia coli*. Science. 1969; 164:1067–1070. [PubMed: 4890175]

Kaberdin VR. Probing the substrate specificity of *Escherichia coli* RNase E using a novel oligonucleotide-based assay. Nucleic Acids Res. 2003; 31:4710–4716. [PubMed: 12907711]

Kole R, Altman S. Properties of purified ribonuclease P from *Escherichia coli*. Biochemistry. 1981; 20:1902–1906. [PubMed: 6164392]

Lee CR, Kim M, Park YH, Kim YR, Seok YJ. RppH-dependent pyrophosphohydrolysis of mRNAs is regulated by direct interaction with DapF in *Escherichia coli*. Nucleic Acids Res. 2014; 42:12746–12757. [PubMed: 25313159]

Lin-Chao S, Wong TT, McDowall KJ, Cohen SN. Effects of nucleotide sequence on the specificity of *rne*-dependent and RNase E-mediated cleavages of RNA I encoded by the pBR322 plasmid. J Biol Chem. 1994; 269:10797–10803. [PubMed: 7511607]

Luciano DJ, Hui MP, Deana A, Foley PL, Belasco KJ, Belasco JG. Differential control of the rate of 5′-end-dependent mRNA degradation in *Escherichia coli*. J Bacteriol. 2012; 194:6233–6239. [PubMed: 22984254]

Mackie GA. Ribonuclease E is a 5′-end-dependent endonuclease. Nature. 1998; 395:720–723. [PubMed: 9790196]

Maitra U, Novogrodsky A, Baltimore D, Hurwitz J. The identification of nucleoside triphosphate ends on RNA formed in the RNA polymerase reaction. Biochem Biophys Res Commun. 1965; 18:801–811.

McDowall KJ, Lin-Chao S, Cohen SN. A+U content rather than a particular nucleotide order determines the specificity of RNase E cleavage. J Biol Chem. 1994; 269:10790–10796. [PubMed: 7511606]

Meyer KD, Patil DP, Zhou J, Zinoviev A, Skabkin MA, Elemento O, Pestova TV, Qian SB, Jaffrey SR. 5′ UTR m^6A promotes cap-independent translation. Cell. 2015; 163:999–1010. [PubMed: 26593424]

Mossessova E, Lima CD. Ulp1-SUMO crystal structure and genetic analysis reveal conserved interactions and a regulatory element essential for cell growth in yeast. Mol Cell. 2000; 5:865–876. [PubMed: 10882122]

Neidhardt FC, Bloch PL, Smith DF. Culture medium for enterobacteria. J Bacteriol. 1974; 119:736–747. [PubMed: 4604283]

Nudler E, Gusarov I, Bar-Nahum G. Methods of walking with the RNA polymerase. Methods Enzymol. 2003; 371:160–169. [PubMed: 14712698]

Pei Y, Shuman S. Interactions between fission yeast mRNA capping enzymes and elongation factor Spt5. J Biol Chem. 2002; 277:19639–19648. [PubMed: 11893740]

Richards J, Belasco JG. Distinct requirements for 5′-monophosphate-assisted RNA cleavage by *Escherichia coli* RNase E and RNase G. J. Biol. Chem. 2016; 291:5038–5048.

Richards J, Luciano DJ, Belasco JG. Influence of translation on RppH-dependent mRNA degradation in *Escherichia coli*. Mol Microbiol. 2012; 86:1063–1072. [PubMed: 22989003]

Ritz C, Spiess AN. qpcR: an R package for sigmoidal model selection in quantitative real-time polymerase chain reaction analysis. Bioinformatics. 2008; 24:1549–1551. [PubMed: 18482995]

Schwartz S. Cracking the epitranscriptome. RNA. 2016; 22:169–174. [PubMed: 26787305]

Shuman S. Structure, mechanism, and evolution of the mRNA capping apparatus. Prog Nucleic Acid Res Mol Biol. 2001; 66:1–40. [PubMed: 11051760]

Shuman S, Hurwitz J. Mechanism of mRNA capping by vaccinia virus guanylyltransferase: characterization of an enzyme--guanylate intermediate. Proc Natl Acad Sci USA. 1981; 78:187–191. [PubMed: 6264433]

Szeberényi J, Roy MK, Apirion D. 7 S RNA: a single site substrate for the RNA processing enzyme ribonuclease E of *Escherichia coli*. Biochim Biophys Acta. 1983; 740:282–290. [PubMed: 6347257]

Tock MR, Walsh AP, Carroll G, McDowall KJ. The CafA protein required for the 5′-maturation of 16 S rRNA is a 5′-end-dependent ribonuclease that has context-dependent broad sequence specificity. J Biol Chem. 2000; 275:8726–8732. [PubMed: 10722715]

Vasilyev N, Serganov A. Structures of RNA complexes with the *Escherichia coli* RNA pyrophosphohydrolase RppH unveil the basis for specific 5′-end-dependent mRNA decay. J Biol Chem. 2015; 290:9487–9499. [PubMed: 25657011]

Vasilyev N, Serganov A. Preparation of short 5′-triphosphorylated oligoribonucleotides for crystallographic and biochemical studies. Methods Mol Biol. 2016; 1320:11–20. [PubMed: 26227034]

Wang D, Shatkin AJ. Synthesis of Gp4N and Gp3N compounds by guanylyltransferase purified from yeast. Nucleic Acids Res. 1984; 12:2303–2315. [PubMed: 6324112]

Wang X, Lu Z, Gomez A, Hon GC, Yue Y, Han D, Fu Y, Parisien M, Dai Q, Jia G, et al. N6-methyladenosine-dependent regulation of messenger RNA stability. Nature. 2014; 505:117–120. [PubMed: 24284625]

Wang X, Zhao BS, Roundtree IA, Lu Z, Han D, Ma H, Weng X, Chen K, Shi H, He C. N^6-methyladenosine modulates messenger RNA translation efficiency. Cell. 2015; 161:1388–1399. [PubMed: 26046440]

Yu L, Shuman S. Mutational analysis of the RNA triphosphatase component of vaccinia virus mRNA capping enzyme. J Virol. 1996; 70:6162–6168. [PubMed: 8709242]

Highlights

- *E. coli* RppH prefers diphosphorylated RNAs to their triphosphorylated counterparts.
- An assay was devised to detect and quantify diphosphorylated RNA 5′ ends.
- Diphosphorylated 5′ ends were found to be abundant on mRNA in *E. coli*.
- 5′-end-dependent RNA decay begins with sequential removal of the γ and β phosphates.

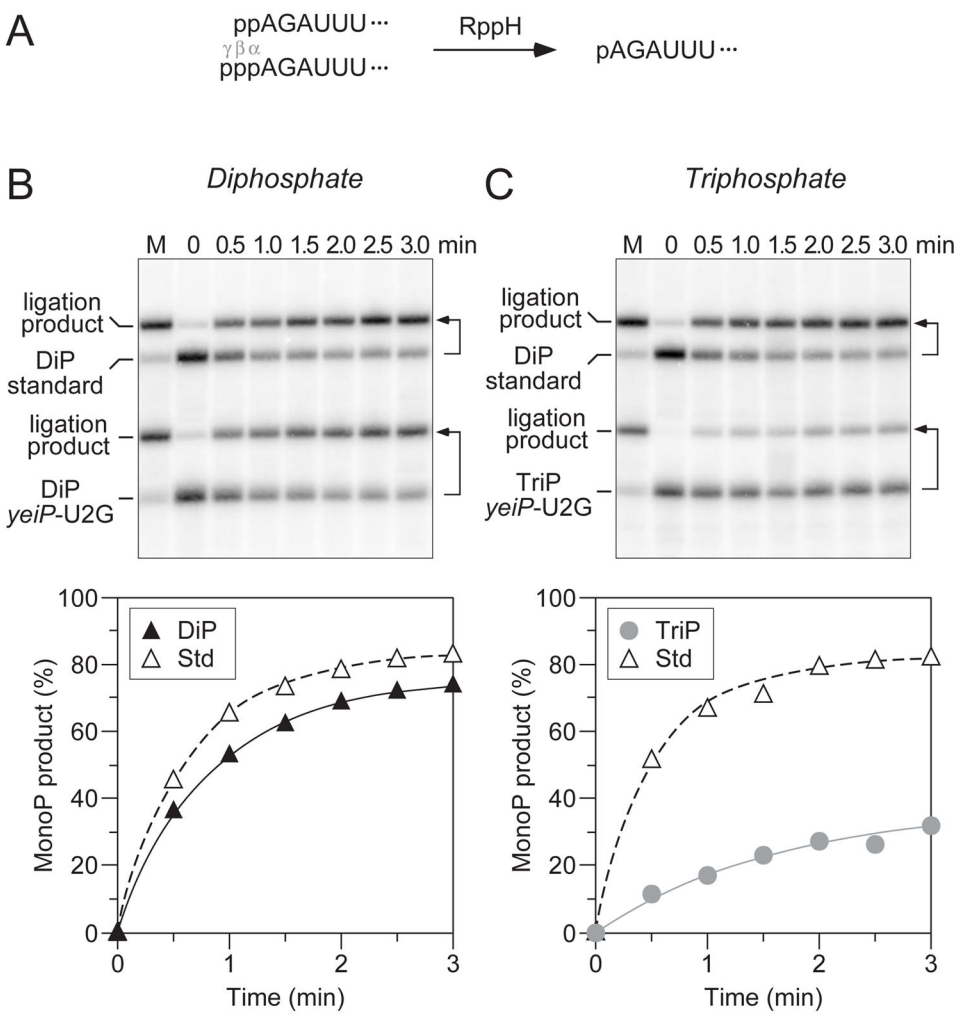

Figure 1. Relative reactivity of diphosphorylated and triphosphorylated RNA as substrates of purified *E. coli* RppH

(A) Substrates and product of the reaction of RppH with diphosphorylated and triphosphorylated *yeiP*-U2G RNA. The first six nucleotides of *yeiP*-U2G are shown. p, 5′-terminal α, β, or γ phosphate. (B, C) The reaction of diphosphorylated and triphosphorylated *yeiP*-U2G with RppH was compared in the presence of the ancillary factor DapF by using PABLO to detect the monophosphorylated reaction products. In each case, a diphosphorylated derivative of *yeiP*-U2G with the same 5′-terminal sequence but a distinct length served as an internal standard. The increase in the concentration of monophosphorylated reaction products is graphed beneath each blot. Representative experiments are shown. Bent arrows beside the blots lead from each RNA substrate to its PABLO ligation product. M, fully monophosphorylated *yeiP*-U2G generated by treating an equivalent substrate mixture with excess RppH for an extended period of time. Filled triangles, reaction of diphosphorylated *yeiP*-U2G (DiP). Gray circles, reaction of triphosphorylated *yeiP*-U2G (TriP). Empty triangles, reaction of the diphosphorylated internal standard (Std). In multiple experiments of this kind, the initial reaction rate of diphosphorylated *yeiP*-U2G was 3.2 ± 0.6 times that of its triphosphorylated counterpart;

because the reactions slowed as a function of time, this value represents a lower limit on the difference in the initial rates.

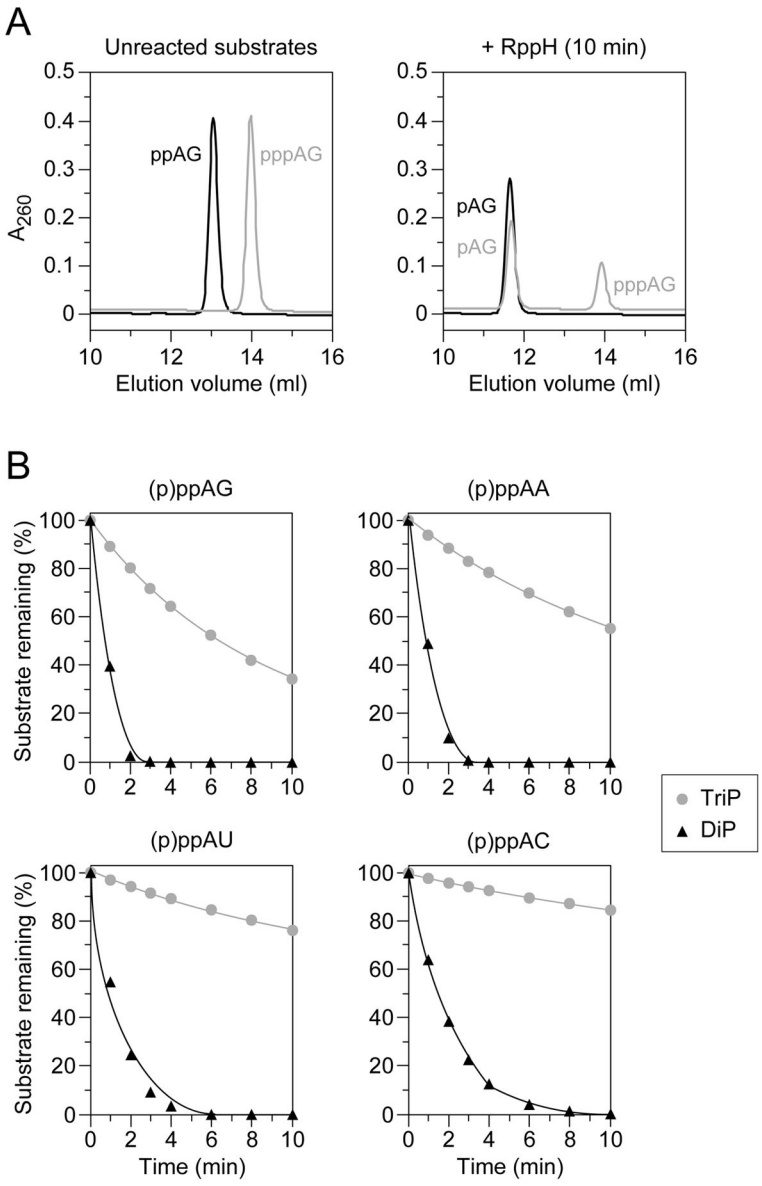

Figure 2. Sequence-independent preference of purified *E. coli* RppH for diphosphorylated over triphosphorylated dinucleotide substrates

(A) Chromatographic separation of diphosphorylated and triphosphorylated AG dinucleotide substrates from monophosphorylated reaction products. Representative samples of separate reactions were quenched before and 10 min after adding RppH and fractionated by anion-exchange chromatography. Substrates and products were detected spectrophotometrically as a function of elution volume, and the chromatographic traces were superimposed. Black traces, reaction of the diphosphorylated substrate (ppAG) to produce a monophosphorylated product (pAG). Gray traces, reaction of the triphosphorylated substrate (pppAG) to produce a monophosphorylated product (pAG).

(B) Relative reactivity of diphosphorylated versus triphosphorylated AG, AA, AU, and AC dinucleotides. Reaction samples were quenched at 1- to 2-min intervals after adding equal amounts of RppH and analyzed chromatographically to determine the percentage of

substrate remaining. Black triangles, reaction of diphosphorylated substrates (DiP). Gray circles, reaction of triphosphorylated substrates (TriP). Mean values from multiple experiments are plotted. To avoid obscured error bars, the standard deviation of each measurement is reported in Table S1.

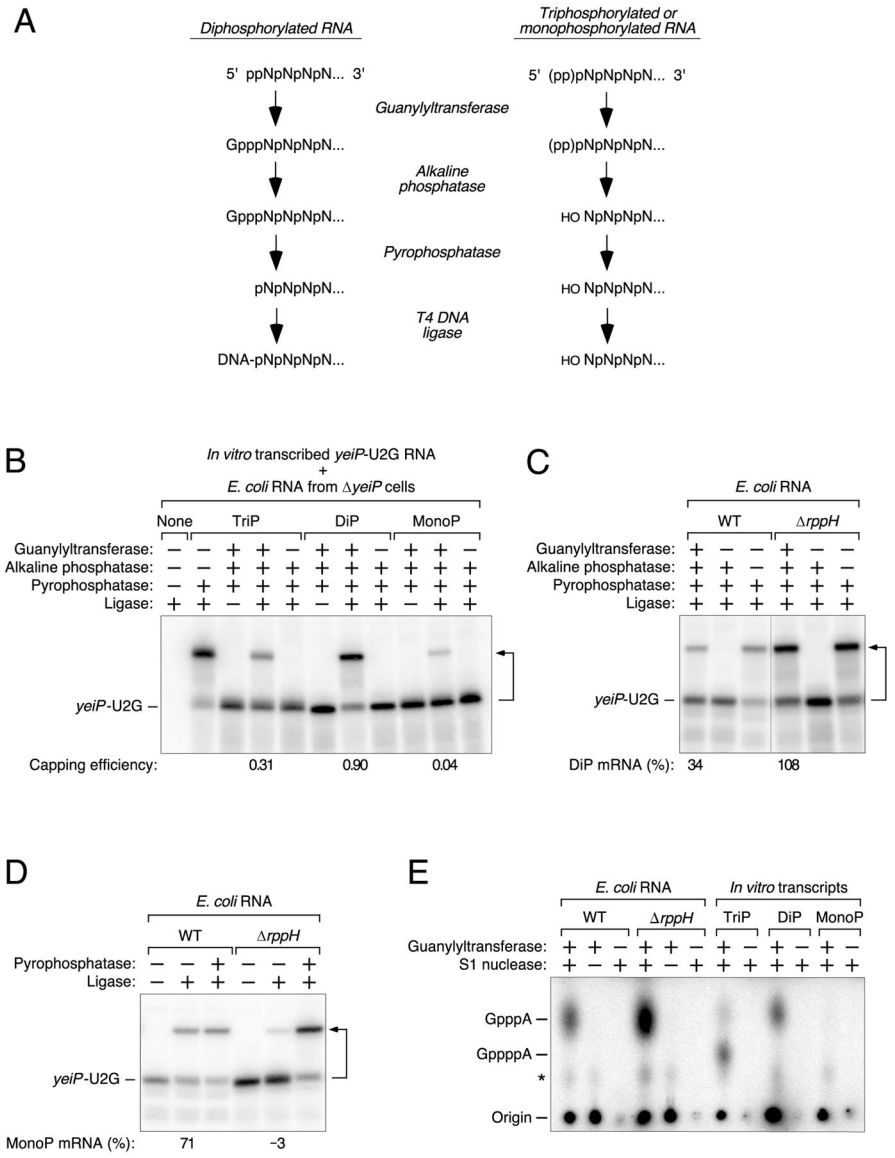

Figure 3. Detection of diphosphorylated *yeiP-U2G* mRNA in *E. coli*

(A) Method for detecting diphosphorylated RNA (PACO). Pce1 preferentially guanylylates the 5′ end of diphosphorylated RNA. Subsequent treatment with alkaline phosphatase removes the exposed 5′-terminal phosphates of triphosphorylated and monophosphorylated RNA but not the protected phosphates of guanylylated RNA, which is then converted to monophosphorylated RNA by treatment with a pyrophosphatase and detected by PABLO. (B) Specificity of PACO as determined by analysis of *in vitro* transcribed *yeiP*-U2G RNA bearing a 5′-terminal triphosphate (TriP), diphosphate (DiP), or monophosphate (MonoP). The analytical reactions were performed in the presence of total *E. coli* RNA from *ΔyeiP* cells to simulate the assay of an endogenous *E. coli* transcript. See also Tables S2 and S3. (C) Relative abundance of diphosphorylated *yeiP*-U2G mRNA in wild-type (WT) and *ΔrppH* cells, as determined by PACO. A vertical line marks the location of superfluous lanes omitted from the image. See also Tables S4 and S5 and Figures S2 and S4.

(D) Relative abundance of monophosphorylated *yeiP*-U2G mRNA in wild-type (WT) and *ΔrppH* cells, as determined by PABLO. See also Tables S4 and S5 and Figures S1 and S4. (E) Number of phosphates in the *yeiP*-U2G cap after guanylylation by Pce1. Equimolar amounts of triphosphorylated, diphosphorylated, or monophosphorylated *yeiP*-U2G standards synthesized by *in vitro* transcription and *yeiP*-U2G mRNA selectively purified from total RNA that had been extracted from wild-type or *ΔrppH* cells were capped by Pce1 in the presence of [α-^{32}P]GTP, digested with nuclease S1 to release the capped 5′-terminal nucleotide, treated with alkaline phosphatase to hydrolyze the remaining GTP, and analyzed by thin layer chromatography on PEI-cellulose and autoradiography. The radiolabeled reaction products comigrated with unlabeled samples of GpppA and GppppA that were obtained commercially and detected by their ability to quench fluorescence (not shown). Capping and subsequent hydrolysis of the diphosphorylated standard produced GpppA. Capping and subsequent hydrolysis of the triphosphorylated standard produced primarily GppppA, along with a small quantity of GpppA whose mechanism of formation is unclear. *, GppppG produced by Pce1-catalyzed capping of GTP (Wang and Shatkin, 1984); Origin, denatured reaction intermediate comprising [α-^{32} P]guanylate covalently bonded to Pce1 (Shuman and Hurwitz, 1981).

For a detailed explanation of how the values in panels B, C, and D were calculated, see STAR Methods. Minor discrepancies versus the theoretical maximum (100%) or minimum (0%) resulted from the small mathematical correction factors that were used and are either within the margin of error or close to it. A bent arrow leads from each RNA substrate to its ligation product.

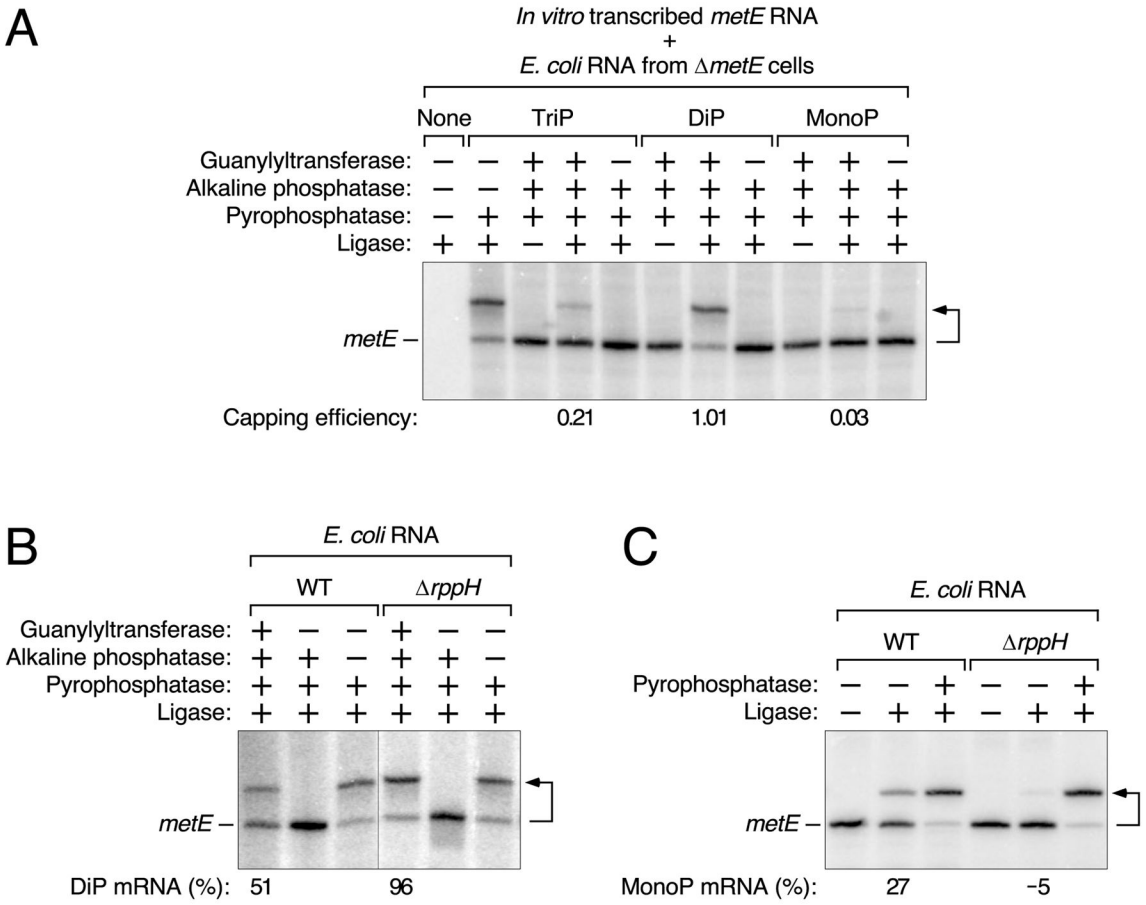

Figure 4. Detection of diphosphorylated *metE* mRNA in *E. coli*

(A) Examination of *in vitro* transcribed *metE* standards bearing a 5′-terminal triphosphate (TriP), diphosphate (DiP), or monophosphate (MonoP) by PACO. The reactions were performed in the presence of total *E. coli* RNA from *ΔmetE* cells. See also Tables S2 and S3.

(B) Relative abundance of diphosphorylated *metE* mRNA in wild-type (WT) and *ΔrppH* cells, as determined by PACO. A vertical line marks the location of superfluous lanes omitted from the image. See also Tables S4 and S5.

(C) Relative abundance of monophosphorylated *metE* mRNA in wild-type (WT) and *ΔrppH* cells, as determined by PABLO. See also Tables S4 and S5 and Figures S1 and S3.

For a detailed explanation of how the values in panels A, B, and C were calculated, see STAR Methods. Minor discrepancies versus the theoretical maximum (100%) or minimum (0%) resulted from the small mathematical correction factors that were used and are either within the margin of error or close to it. A bent arrow leads from each RNA substrate to its ligation product.

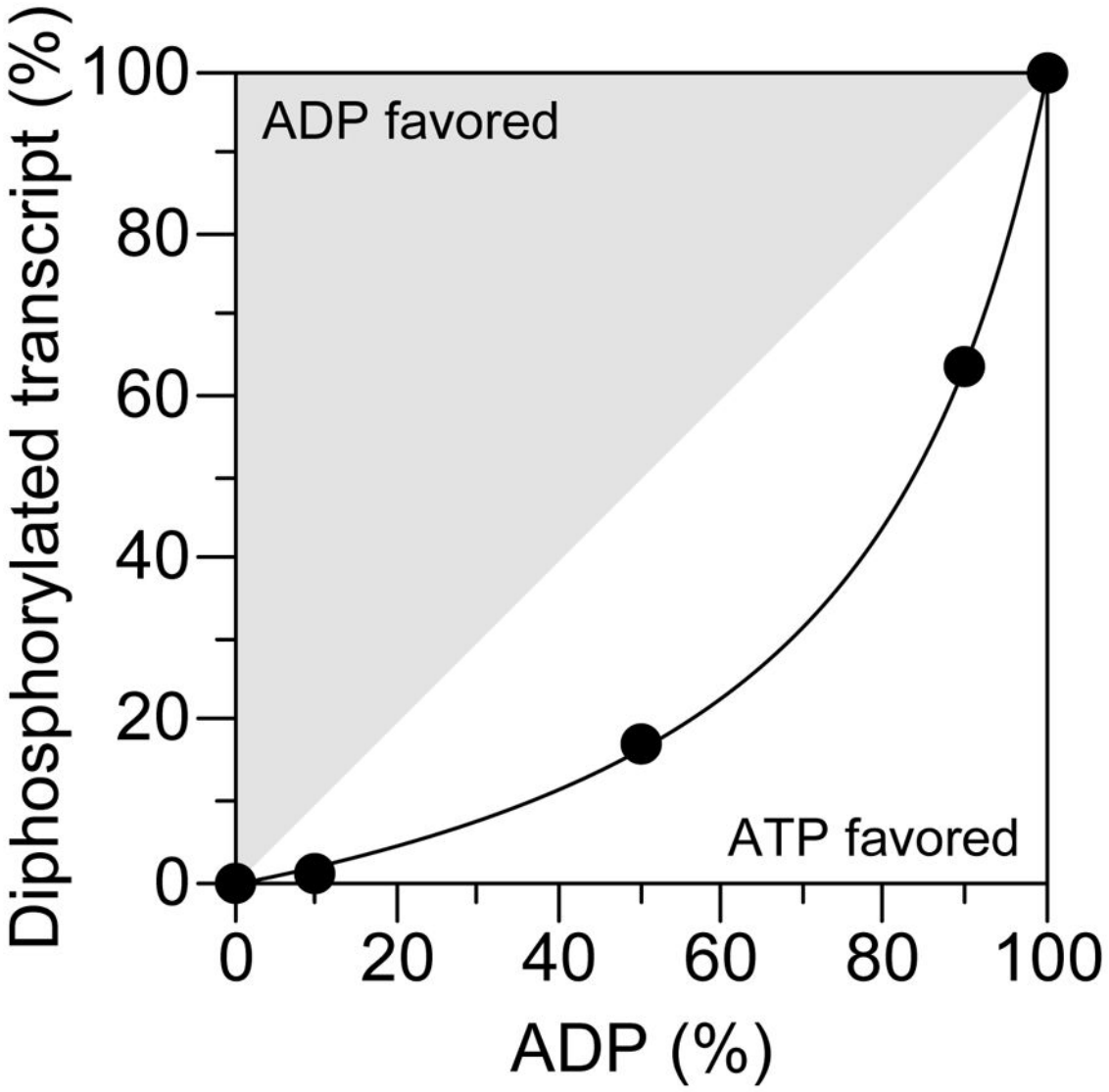

Figure 5. Competitive incorporation of ADP and ATP at the 5′ end of transcripts synthesized by *E. coli* RNA polymerase

EcIVTa RNA (5′ AUCUUUCUCUGUUGUUCUUCUGUUGGUCUUUUUCCCUGCCCUGUGCGGUCGG CGUUGCGUUCGGU 3′) was synthesized by *E. coli* RNA polymerase at various ADP : ATP ratios, and the relative abundance of diphosphorylated versus triphosphorylated 5′ termini was determined by PACO (filled circles). The PACO ligation yields for RNA synthesized at ratios of 100 : 0 and 0 : 100 (100% diphosphorylated and 100% triphosphorylated EcIVTa, respectively) provided correction factors that allowed precise quantification of the data obtained at intermediate ratios. The curved line represents the relative yield of diphosphorylated EcIVTa that would be expected if ATP is incorporated 5 times more readily than ADP, and the gray and white zones encompass the range of experimental outcomes expected for preferential incorporation of ADP or ATP, respectively.

A representative experiment is shown. The observed preference for 5′-terminal incorporation of ATP versus ADP was 5.0 ± 0.2 (ATP/ADP).

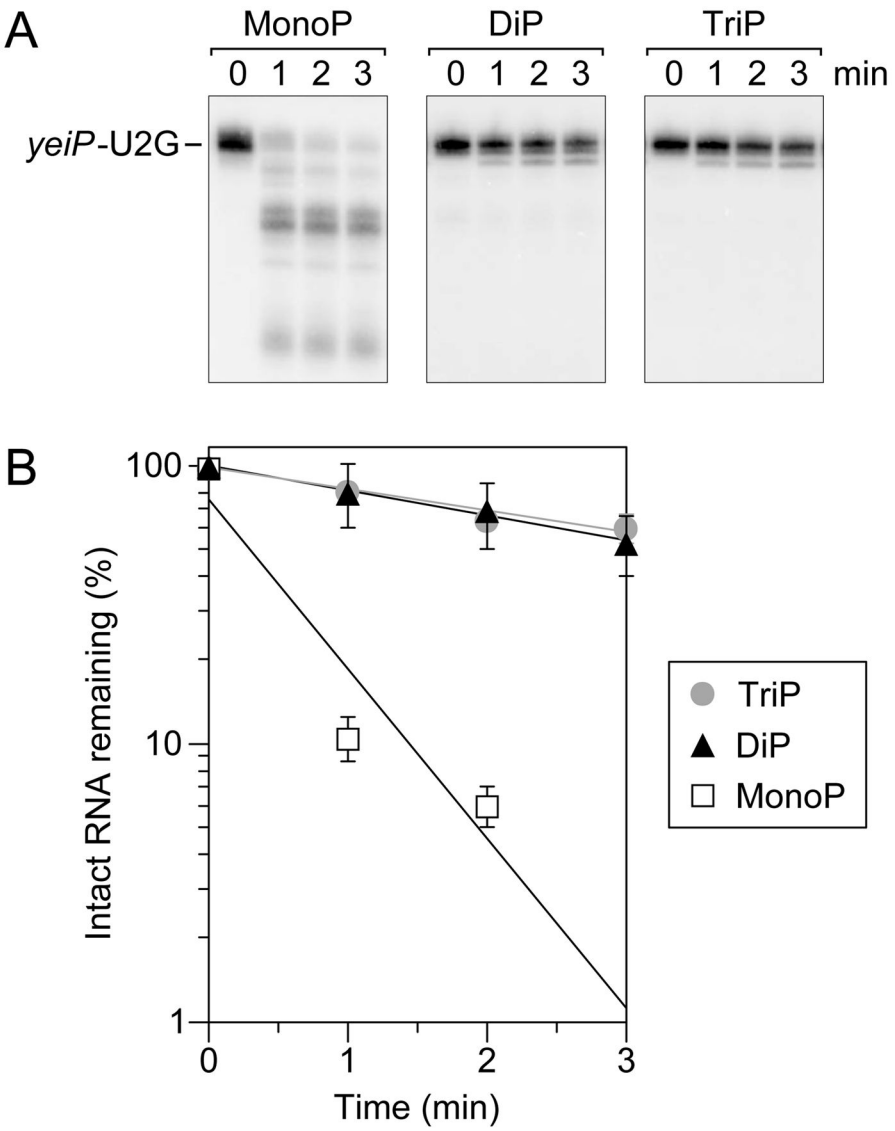

Figure 6. Relative reactivity of diphosphorylated RNA as an RNase E substrate

(A) Reaction of monophosphorylated (MonoP), diphosphorylated (DiP), and triphosphorylated (TriP) *yeiP*-U2G with equal amounts of *E. coli* N-RNase E. Reaction samples were quenched at time intervals and analyzed by Northern blotting.

(B) Semilogarithmic plots of the amount of intact *yeiP*-U2G RNA remaining as a function of time after N-RNase E addition. Empty squares, monophosphorylated *yeiP*-U2G. Filled triangles, diphosphorylated *yeiP*-U2G. Gray circles, triphosphorylated *yeiP*-U2G. Mean values from multiple experiments are plotted. Error bars represent standard deviations.

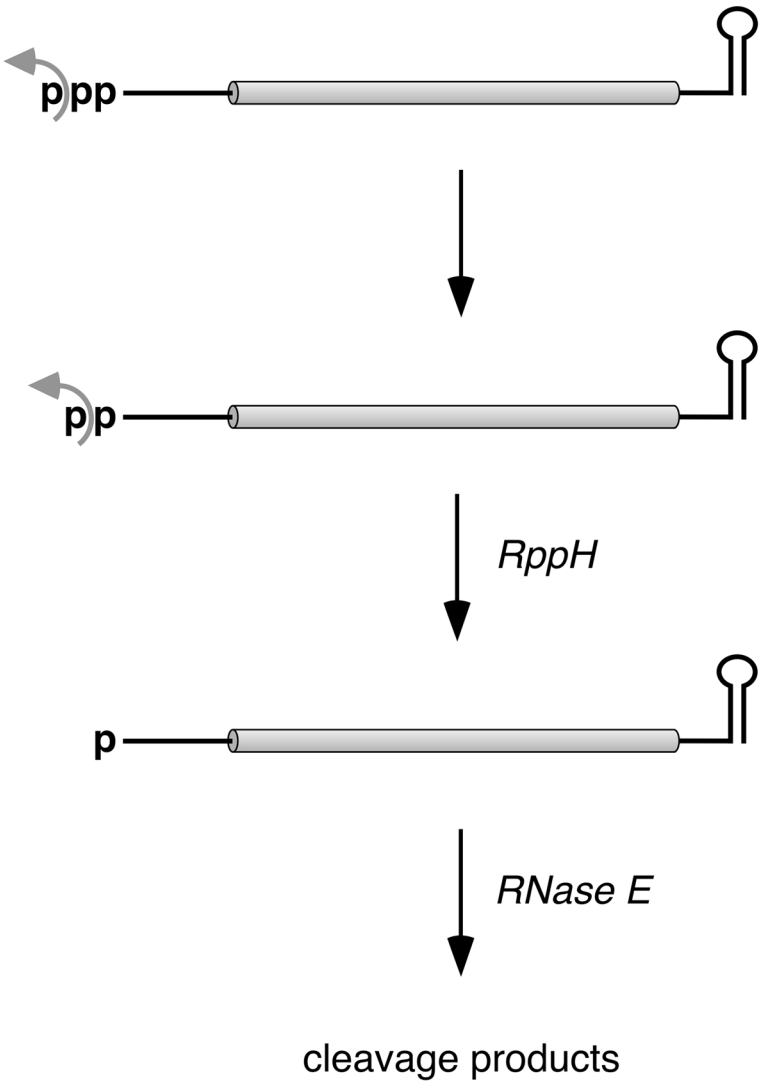

Figure 7. Principal mechanism of 5′-end-dependent RNA degradation in *E. coli*

Swift removal of the γ phosphate of a triphosphorylated primary transcript by an unidentified enzyme generates a 5′-terminal diphosphate susceptible to rapid β phosphate hydrolysis by RppH. Less often, RppH may convert the 5′-terminal triphosphate to a monophosphate in a single step. The monophosphorylated 5′ end of the resulting intermediate binds to a pocket on the surface of RNase E, thereby facilitating endonucleolytic cleavage by this ribonuclease at various downstream locations. The cleavage products are subsequently degraded by the combined action of RNase E and 3′ exonucleases (not shown). Curved arrows represent phosphate removal.